Proceedings of IMECE 2004
2004 ASME International Mechanical Engineering Congress
November 13-19, 2004, Anaheim, California, USA

DRAFT IMECE2004-60129

COMPACT ANALYTICAL MODELS FOR EFFECTIVE THERMAL CONDUCTIVITY OF ROUGH SPHEROID PACKED BEDS

M. Bahrami[1], M. M. Yovanovich[2], and J. R. Culham[3]
Microelectronics Heat Transfer Laboratory,
Deptartment of Mechanical Engineering,
University of Waterloo, Waterloo, ON, Canada N2L 3G1

Abstract

New compact analytical models for predicting the effective thermal conductivity of regularly packed beds of rough spheres immersed in a stagnant gas are developed. Existing models do not consider either the influence of the spheres roughness or the rarefaction of the interstitial gas on the conductivity of the beds. Contact mechanics and thermal analyses are performed for uniform size spheres packed in SC and FCC arrangements and the results are presented in the form of compact relationships. The present model accounts for the thermophysical properties of spheres and the gas, contact load, spheres diameter, spheres roughness and asperities slope, and temperature and pressure of the gas. The present model is compared with experimental data for SC and FCC packed beds and good agreement is observed. The experimental data cover a wide range of the contact load, surface roughness, interstitial gas type, and gas temperature and pressure.

Nomenclature

A	=	area, m^2
a_L	=	radius of macrocontact, m
a_H	=	radius of Hertzian contact, m
b_L	=	chord of macrogap, m
c_1	=	Vickers microhardness coefficient, Pa
c_2	=	Vickers microhardness coefficient
D	=	sphere diameter, m
E	=	Young's modulus, Pa
E'	=	effective elastic modulus, Pa
F_c	=	normal contact force, N
FCC	=	Face Center Close
H^*	=	$c_1 (\sigma'/m)^{c_2}$, Pa
Kn	=	Knudsen number
k	=	thermal conductivity, W/mK
L	=	length, m
m	=	mean absolute surface slope
M	=	gas parameter, m
P	=	pressure, Pa
Pr	=	Prandtl number
Q	=	heat flow rate, W
q	=	heat flux, W/m^2
R	=	thermal resistance, K/W
SC	=	Simple Cubic
T	=	temperature, K

Greek

α	=	non-dimensional parameter, $\equiv \sigma\rho/a_H^2$
α_T	=	thermal accommodation coefficient
γ	=	exponent of general pressure distribution
γ_g	=	ratio of gas specific heats, $\equiv c_p/c_v$
Λ	=	mean free path, m
υ	=	Poisson's ratio
ξ	=	non-dimensional radial position, $\equiv r/a_L$
ρ	=	radius of sphere, m
σ	=	RMS surface roughness, m
σ'	=	σ/σ_0, $\sigma_0 = 1\ \mu m$
τ	=	non-dimensional parameter, $\equiv \rho/a_H$
ω_0	=	bulk normal deformation at origin, m

Subscripts

0	=	reference value, value at origin
1, 2	=	solid 1, 2

[1]Ph.D. Candidate, Department of Mechanical Engineering.
[2]Distinguished Professor Emeritus, Department of Mechanical Engineering. Fellow ASME.
[3]Associate Professor, Director, Microelectronics Heat Transfer Laboratory. Member ASME.

a	=	apparent
BR	=	boundary resistance
c	=	cell
g	=	gas, microgap
G	=	macrogap
H	=	Hertz
j	=	joint
L	=	large, macrocontact
r	=	real
s	=	solid, micro

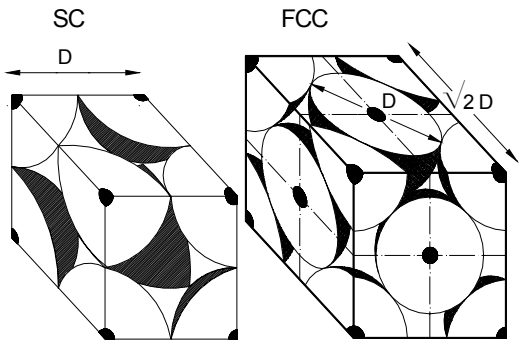

Figure 1. ARRANGMENT FOR SIMPLE CUBIC AND FACE CENTER CLOSE PACKINGS

INTRODUCTION

Packed beds have a wide variety of applications in thermal systems. One of the significant characteristics of packed beds is the high ratio of solid surface area to volume. This property is useful in applications such as catalytic reactors, heat recovery processes, heat exchangers, heat storage systems, the breeder blanket about fusion reactors [1], and insulators. The insulator packed beds are often immersed in a gas at reduced pressure.

The thermal conductivity of packed beds is not isotropic and it is difficult to formulate a model that fully defines the effective thermal conductivity. However, the structure of a packed bed can be modeled assuming regularly packed beds. A regularly packed bed is one in which the same arrangement of spheres, uniform in size, is repeated throughout the bed. Therefore a typical "basic cell" will represent the entire bed. There are three such regular packings: 1) Simple Cubic (SC), 2) Body Center Close (BCC), and 3) Face Center Close (FCC). Tien and Vafai [2] showed that the effective thermal conductivity of a random packed bed filled by a single phase fluid presents two limits. The upper bound can be obtained considering the FCC packing and the lower bound can be represented by the SC packing. Therefore, in this study only the thermal conductivity of the SC and FCC arrangements will be studied. The SC and FCC arrangements for packed beds of uniform diameter spheres are shown in Fig. 1.

Each cell is made up of contact regions. A contact region is composed of a contact area between two portions of spheres, surrounded by a gas layer.

Many studies have been performed on the prediction of thermal conductivity of packed beds filled with stagnant gas. The existing models can be categorized into two main groups. The first is numerical models, e.g. finite element methods (FEM) which can treat the three dimensional problem by dividing the bed into many cells with temperature and heat flow matched at their boundaries. One should keep in mind that it is a combined thermal and mechanical three dimensional numerical analysis which makes the FEM modeling extremely expensive from the calculative point of view [3]. Additionally, employing a numerical approach makes it difficult to extract the relative importance of different conduction paths from such computer software. Also, thermal contact resistance (TCR) of rough spheres must be fed into the software as boundary conditions when commercial FEM software is used, thus the TCR problem must be solved separately. Buonanno and Carotenuto [4] used a three dimensional FEM model to evaluate the thermal conductivity of simple cubic and body centered cubic packed beds and compared their model with experimental data collected by others. Buonanno et al. [3] and [5] conducted experiments and measured the effective thermal conductivity of uniformly sized rough stainless steel spheres. Their packed bed was filled with air at atmospheric pressure and 20° C temperature. They compared their experimental data with their FEM numerical model and showed good agreement with the data. However, Buonanno et al. [3] did not report any expression or relationship for predicting the thermal conductivity of packed beds. Additionally, they did not compare their model with any data at rarefied gas pressures.

The second group of existing models is the analytical models which break the problem into distinct conduction paths, e.g., the contact area between spheres, the gas layer between spheres, etc.; and calculates the conductivity of the bed as a series/parallel combination of the individual resistances for these paths. The advantage of the analytical approach is that it enables one to evaluate easily the relative contributions and trends of each conduction path as a function of the packed bed parameters/properties. Different approaches were taken by researchers developing analytical models, some researchers such as Slavin et al. [6] assumed that the contact between two spheres is essentially a point contact and the heat transfer through the contact region can be ignored for hard materials. Ogniewicz and Yovanovich [7] and Turyk and Yovanovich [8] developed analytical models

for predicting the effective thermal conductivity of the basic cells of packed beds of uniformly sized spheres and compared their models with experimental data. These models were limited to smooth spheres.

To the authors' knowledge there are no analytical models for predicting the thermal conductivity of packed beds which take into account the effect of surface roughness and rarefaction of the interstitial gas simultaneously. The objective of this work is to develop an analytical compact model for packed beds of identical rough spheres immersed in a stagnant gas at gas pressure varying from atmospheric to vacuum and under various mechanical loads. The trends predicted by the present model allows one to study the effect of important input variables involved in real packed beds. It also provides design tools for predicting and improving upon the thermal performance of random packed beds.

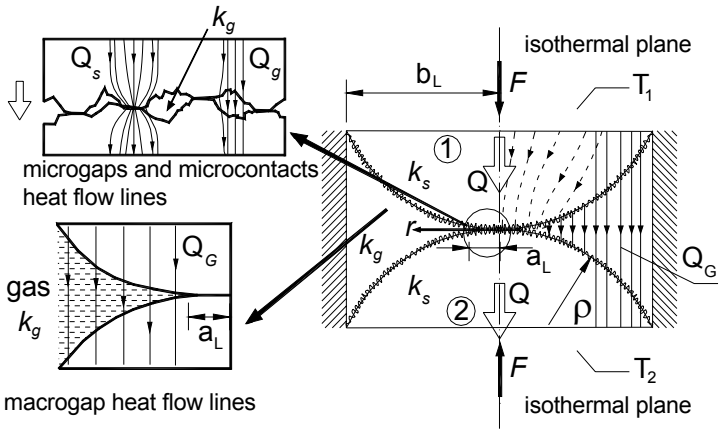

Figure 2. CONTACT OF ROUGH SPHERES WITH PRESENCE OF INTERSTITIAL GAS

THEORETICAL BACKGROUND

Modeling the thermal conductivity of spherical packed beds includes two main analyses i) conduction between rough spheres and ii) heat transfer through interstitial stagnant gas between solids. The geometry of a general joint is shown in Fig. 2, where two spherical caps are placed in mechanical contact. The gap between the contacting bodies is filled with a stagnant gas at pressure P_g and temperature T_g and heat is transferred from one sphere to another. Thermal energy can be transferred across the joint via three distinct modes: radiation, conduction through interstitial gas in the gap, and conduction through the real contact area. Thermal radiation across the gap remains small as long as the surface temperatures are not too high and in most applications can be neglected [9]. Natural convection does not occur within in the gap when the Grashof number is less than 2500 [10]. In practical situations concerning packed beds, the Grashof number is less than 2500, thus the heat transfer through natural convection is small and can be neglected. Therefore, the remaining heat transfer modes are conduction through the microcontacts and conduction through the interstitial gas filling the gap between contacting bodies.

A study of the heat conduction between contacting rough spheres is the first step toward modeling the heat transfer in packed beds. A contact region is the basic element that creates the packed beds. The heat transferred in an isolated contact region determines the thermal behavior of the entire bed. As schematically shown in Fig. 2, conduction occurs through three main paths, the interstitial gas within the microgap Q_g, microcontacts Q_s, and the interstitial gas within the macrogap Q_G. As a result of the small real contact area [11] and low thermal conductivities of interstitial gases, heat flow experiences a relatively large thermal resistance passing through the joint, this phenomenon leads to a relatively high temperature drop across the joint.

The thermal joint resistance of rough spherical surfaces with the presence of an interstitial gas contains four thermal resistance components, 1) the macrocontact constriction/spreading resistance R_L, 2) the microcontacts constriction/spreading resistance R_s, 3) resistance of the interstitial gas in the microgap R_g, and 4) the resistance of interstitial gas in the macrogap R_G. Figure 3 presents the thermal resistance network for a spherical rough joint with the presence of an interstitial gas that is used in this study. As shown, the macrogap provides a parallel path for conduction between the two isothermal planes, therefore the joint resistance can be calculated from

$$R_j = \left[\frac{1}{(1/R_s + 1/Rg)^{-1} + R_L} + \frac{1}{R_G} \right]^{-1} \qquad (1)$$

As shown in Fig. 3, R_G has three components: the macrogap resistance and R_1 and R_2 corresponding to the bulk thermal resistance of the solid layers in spheres 1 and 2, respectively. The solid layers bulk resistances, R_1 and R_2, are negligible compared to R_G since the gas thermal conductivity is much smaller than the thermal conductivity of the solids, i.e., $k_g \ll k_s$.

The above thermal resistances are discussed and simple correlations are proposed for calculating each resistance in the following sections.

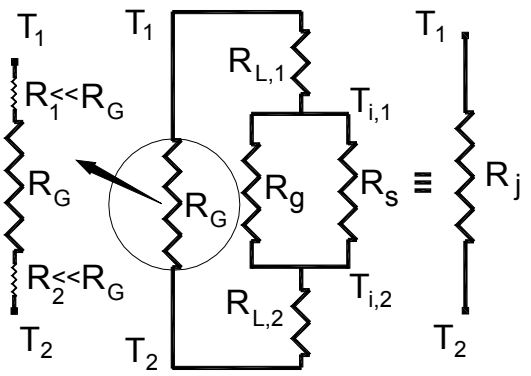

Figure 3. THERMAL RESISTANCE NETWORK, SPHERICAL ROUGH JOINTS IN PRESENCE OF GAS

Microcontacts Thermal Resistance, $\mathbf{R}_s$

Engineering (real) surfaces have roughness. If the asperities of a surface are isotropic and randomly distributed over the surface, the surface is called Gaussian. When random rough surfaces are placed in mechanical contact, *real* contact occurs at the top of the surface asperities called microcontacts. The microcontacts are distributed randomly in the apparent contact area or the macrocontact area. They are located far from each other. The real contact area A_r, the summation of the microcontacts, forms a small portion of the nominal contact area, typically a few percent of the nominal contact area. The contact between two Gaussian rough surfaces is modeled by the contact between a single Gaussian surface that has the combined surface characteristics with a perfectly smooth surface, for more detail see [12]. The combined roughness σ and surface slope m can be found from

$$\sigma = \sqrt{\sigma_1^2 + \sigma_2^2} \quad \text{and} \quad m = \sqrt{m_1^2 + m_2^2} \tag{2}$$

The microcontacts are often assumed to be isothermal [12]. Thermal constriction/spreading resistance of microcontacts can be modeled using a flux tube geometry [13] or if microcontacts are considered to be located far enough from each other, the isothermal heat source on a half-space solution [9] can be used. Bahrami et al. [14] compared these solutions and showed that the microcontacts can be considered as heat sources on a half-space for most engineering applications. Bahrami et al. [14] assumed plastically deformed asperities and used scale analysis techniques and developed a compact model to predict the thermal constriction/spreading resistance through the microcontacts, R_s

$$R_s = \frac{0.565 H^* (\sigma/m)}{k_s F} \tag{3}$$

where,

$$k_s = \frac{2k_1 k_2}{k_1 + k_2} \quad H^* = c_1 \left(\frac{\sigma'}{m}\right)^{c_2}$$

where $\sigma' = \sigma/\sigma_0$ and $\sigma_0 = 1\ \mu m$, c_1, c_2, k_s, and F are a reference value, correlation coefficients determined from the Vickers microhardness measurements [9], the harmonic mean of solid thermal conductivities, and the applied load, respectively. Yovanovich and Hegazy [15] showed through experiments that the surface microhardness is much higher than the bulk hardness and that the microhardness decreases until the bulk hardness is reached. They proposed a correlation for determining the microhardness, $H_{mic} = c_1 \left(d_v/\sigma_0\right)^{c_2}$, where $d_v\ \mu m$ is the Vickers indentation diagonal. Sridhar and Yovanovich [16] suggested empirical relations to estimate Vickers microhardness coefficients, using the bulk hardness of the material. Two least-square-cubic fit expressions were reported

$$\begin{aligned} c_1 &= H_{BGM}\left(4.0 - 5.77\kappa + 4.0\kappa^2 - 0.61\kappa^3\right) \\ c_2 &= -0.57 + 0.82\kappa - 0.41\kappa^2 + 0.06\kappa^3 \end{aligned} \tag{4}$$

where $\kappa = H_B/H_{BGM}$, H_B is the Brinell hardness of the bulk material, and $H_{BGM} = 3.178\ GPa$. The above correlations are valid for the range $1.3 \le H_B \le 7.6\ GPa$. In situations where an effective value of microhardness H_{mic} is known, the Vickers microhardness coefficients will be $c_1 = H_{mic}$ and $c_2 = 0$.

Macrocontact Thermal Resistance, $\mathbf{R}_L$

Bahrami et al. [17] studied mechanical contact of spherical rough surfaces. A closed set of governing relationships was reported for spherical rough contacts and solved numerically. The actual contact geometry of the spheres was replaced by a flat surface and a profile, which resulted in the same undeformed gap between the surfaces [18]. Similar to the Hertzian theory and Greenwood and Tripp [19], the spherical profile was approximated by a paraboloid in the contact region. Also the contact was assumed to be frictionless, i.e., it was assumed that there were no tangential forces in the contact area. The bulk deformation was assumed to be within the elastic limit of the solids and the microcontacts were assumed to deform plastically. All elastic deformations were considered to occur in one body, which had an effective elastic modulus and the other body was assumed to be rigid. The effective elastic modulus and the equivalent radius of curvature can be found from

$$\begin{aligned} \frac{1}{\rho} &= \frac{1}{\rho_1} + \frac{1}{\rho_2} \\ \frac{1}{E'} &= \frac{1-\upsilon_1^2}{E_1} + \frac{1-\upsilon_2^2}{E_2} \end{aligned} \tag{5}$$

Bahrami et al. [17] proposed a general contact pressure distribution which covers the entire range of spherical rough contacts including the Hertzian smooth limit. Simple correlations were developed for the maximum contact pressure P_0 and the radius of the macrocontact area a_L. Applying the Buckingham Π theorem, it was shown that there are two important governing non-dimensional parameters α and τ that describe the contact problem. The non-dimensional roughness parameter α, defined by Greenwood et al. [20], is the ratio of roughness over the Hertzian maximum bulk deformation, $\omega_{0,H}$

$$\alpha = \frac{\sigma}{\omega_{0,H}} \equiv \frac{\sigma\rho}{a_H^2} = \sigma\left(\frac{16\rho E'^2}{9F^2}\right)^{1/3} \tag{6}$$

where $a_H = (0.75F\rho/E')^{1/3}$ is the Hertzian radius of contact, i.e., the limiting contact case where both surfaces are ideally smooth. The other non-dimensional parameter was chosen as

$$\tau = \frac{\rho}{a_H} = \left(\frac{4E'\rho^2}{3F}\right)^{1/3} \tag{7}$$

The general pressure distribution is [17]

$$P(\xi) = P_0\left(1-\xi^2\right)^{\gamma} \tag{8}$$

$$P_0' = \frac{P_0}{P_{0,H}} = \frac{1}{1+1.37\alpha\,\tau^{-0.075}} \tag{9}$$

$$\frac{a_L}{a_H} = \begin{cases} 1.605/\sqrt{P_0'} & 0.01 \le P_0' \le 0.47 \\ 3.51 - 2.51P_0' & 0.47 \le P_0' \le 1 \end{cases} \tag{10}$$

where $P_{0,H} = 1.5F/\pi a_H^2$, $\xi = r/a_L$, and $\gamma = 1.5\,(P_0/P_{0,H})\,(a_L/a_H)^2 - 1$ are the maximum Hertzian contact pressure, non-dimensional radial position, and the general pressure distribution exponent, respectively. The proposed model was compared with more than 220 experimental data points collected by others and good agreement was observed [17]. The RMS difference between the radius of the macrocontact predicted by the model and the data was reported to be approximately 6.2 percent.

Yovanovich et al. [21] studied the thermal spreading resistance of a heat source on a sphere with different boundary conditions. They showed that for relatively small contact radii, compared to the radius of the sphere, the constriction resistance of the contact region is approximately equal to the constriction resistance of a heat source on a half space. In this study, it is assumed that the macrocontact region is isothermal. Therefore, the macrocontact constriction/spreading resistance is

$$R_L = \frac{1}{2k_s a_L} \tag{11}$$

where a_L is calculated using Eq. (10).

Conduction Through Gas, $\mathbf{R}_g$ and $\mathbf{R}_G$

Conduction heat transfer in a gas layer between two parallel plates is commonly divided into four heat-flow regimes [22]: continuum, temperature-jump or slip, transition, and free-molecular. The parameter that characterizes the regimes is the Knudsen number, $Kn = \Lambda/d$, where Λ and d are the molecular mean free path and the distance separating the two plates, respectively. The molecular mean free path is defined as the average distance a gas molecule travels before it collides with another gas molecule and it is proportional to the gas temperature and inversely proportional to the gas pressure [23]

$$\Lambda = \frac{P_0}{P_g}\frac{T_g}{T_0}\,\Lambda_0 \tag{12}$$

where Λ_0 is the mean free path value at some reference gas temperature and pressure T_0 and P_0. The heat transfer in a gas layer between two isothermal plates for all four flow regimes can be effectively calculated from [23]

$$q_g = \frac{k_g}{d+M}\left(T_1 - T_2\right) \tag{13}$$

where T_1, T_2, d, k_g, and q_g are the uniform temperatures and the distance between the two *isothermal* parallel plates, gas thermal conductivity, and the gap heat flux, respectively. The gas parameter M is defined as

$$M = \left(\frac{2-\alpha_{T1}}{\alpha_{T1}} + \frac{2-\alpha_{T2}}{\alpha_{T2}}\right)\left(\frac{2\gamma_g}{1+\gamma_g}\right)\frac{1}{\mathrm{Pr}}\,\Lambda \tag{14}$$

where α_{T1}, α_{T2}, γ_g, and Pr are thermal accommodation coefficients corresponding to the gas-solid combination of plates 1 and 2, ratio of the gas specific heats, and gas Prandtl number, respectively. Thermal accommodation coefficient α_T depends on the type of gas-solid combination and is in general very sensitive to the condition of the solid surfaces. It represents the degree to which the kinetic energy of a gas molecule is exchanged while in collision with the solid wall. Song and Yovanovich [24] purposed a correlation for predicting α_T for engineering surfaces as follows:

$$\alpha_T = \exp\left[-0.57\left(\frac{T_s - T_0}{T_0}\right)\right]\left(\frac{M_g^*}{6.8+M_g^*}\right) + \frac{2.4\mu}{(1+\mu)^2}\left\{1-\exp\left[-0.57\left(\frac{T_s-T_0}{T_0}\right)\right]\right\} \tag{15}$$

where

$$M_g^* = \begin{cases} M_g & \text{for monatomic gases} \\ 1.4M_g & \text{for diatomic/polyatomic gases} \end{cases}$$

where $T_0 = 273\ K$. Equation (15) is general and can be used for any combination of gases and solid surfaces for a wide

temperature range. The agreement between the predicted values and the experimental data is within 25 percent.

The authors developed a compact analytical model for predicting the heat conduction through interstitial gas between rough spherical bodies [25]. The non-conforming region between the solids was divided into infinitesimal surface elements where Eq. (13) could be used. Thermal resistance of the interstitial gas through the microgap and the macrogap were calculated by integrating these surface elements over the macrocontact and the macrogap areas, respectively. The microgap and the macrogap can be represented for the contact of two rough spheres as follows [25]:

$$R_g = \frac{2\sqrt{2}\sigma\ a_2}{\pi k_g a_L^2 \ln\left(1 + \dfrac{a_2}{a_1 + M/\left(2\sqrt{2}\sigma\right)}\right)} \tag{16}$$

where,

$$a_1 = \mathrm{erfc}^{-1}\left(\frac{2P_0}{H'}\right)$$

$$a_2 = \mathrm{erfc}^{-1}\left(\frac{0.03P_0}{H'}\right) - a_1$$

$$R_G = \frac{2}{\pi k_g \left[S \ln\left(\dfrac{S-B}{S-A}\right) + B - A\right]} \tag{17}$$

where $A = 2\sqrt{\rho^2 - a_L^2}$, $B = 2\sqrt{\rho^2 - b_L^2}$, $S = 2(\rho - \omega_0) + M$, $H^{'} = c_1 (1.62\sigma'/m)^{c_2}$, and $\omega_0 = a_L^2/2\rho$. The inverse complementary error function $\mathrm{erfc}^{-1}(x)$ can be determined from [26]

$$\mathrm{erfc}^{-1}(x) = \begin{cases} \dfrac{1}{0.218 + 0.735\ x^{0.173}} & 10^{-9} \le x \le 0.02 \\ \dfrac{1.05\,(0.175)^x}{x^{0.12}} & 0.02 < x \le 0.5 \\ \dfrac{1-x}{0.707 + 0.862x - 0.431x^2} & 0.5 < x \le 1.9 \end{cases} \tag{18}$$

The maximum relative difference between Eq. (18) and $\mathrm{erfc}^{-1}(x)$ is less than 2.8 percent for the range of $10^{-9} \le x \le 1.9$.

CONDUCTION IN BASIC CELLS

The solid fraction ε is the ratio of the solid volume to the total volume of the packed bed, i.e., $\varepsilon = V_s/V$. Table 1 lists the solid fraction for the three typical cells, SC, BCC, and FCC. The solid fraction of a packed bed can be evaluated by weighing the entire bed excluding the container weight. If weight of the bed is W_b, the density of the solids ρ_s, and the volume of the bed V_b, the solid fraction is given by $\varepsilon = W_b/(gV_b\rho_s)$. Figure 4 shows the plan view of these three packing for a packed bed which is formed by spheres of diameter D.

Table 1. SOLID FRACTION AND CELL DIMENSION FOR PACKED BEDS

Packing	**Cell Length $\mathbf{L}_c$**	**Solid Fraction $\boldsymbol{\varepsilon}$**
SC	D	$\pi/6 = 0.524$
BCC	$2\sqrt{3}D/3$	$\sqrt{3}\pi/8 = 0.680$
FCC	$\sqrt{2}D$	$\sqrt{2}\pi/6 = 0.740$

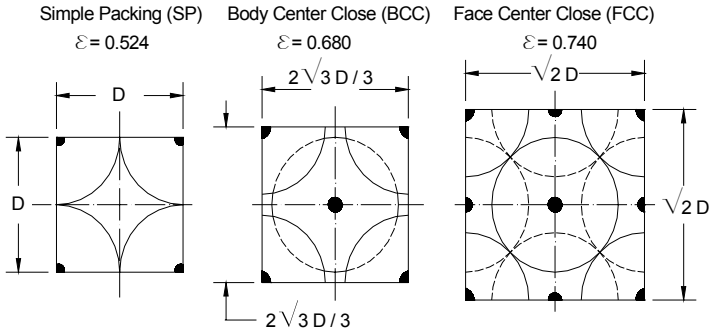

Figure 4. DIMENSIONS AND ARRANGMENTS OF SC, BCC, FCC PACKINGS

Consider a basic cell that has the length L_c and the cross sectional area A_c, as shown in Fig. 5. The top and bottom surfaces are isothermal and the four lateral walls are adiabatic. The applied load is considered as a hydrostatic pressure P_a acting on all the walls. This load can be a result of one or more of the following: the structural load due to the weight of spheres, thermal expansion of the spheres, packing under pressure, exerted external load on the bed, etc.

A real packed bed is a non-homogenous medium of different thermal conductivities corresponding to local variation of apparent load. Depending on this variation, different approaches can be taken to calculate the effective thermal conductivity of the bed. A proper treatment is to integrate the local effective thermal conductivity over the entire bed to find the apparent thermal conductivity. A simpler approach is to consider an average contact load which is constant for all the joints in the bed. This average contact load can be considered as the arithmetic mean between the highest and the lowest contact loads. In this study the latter method is employed to develop compact expressions for the effective thermal conductivity. However, the first method can also be applied using the same approach.

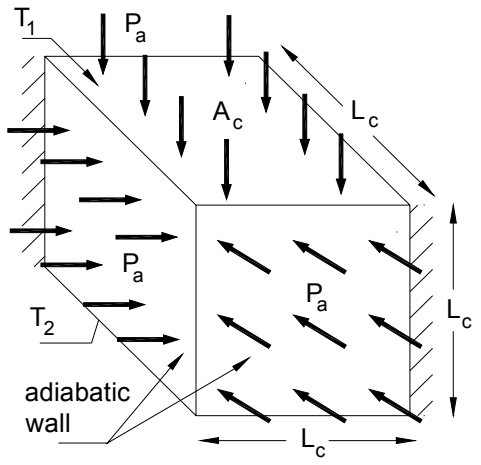

Figure 5. GEOMETRY AND HYDROSTATIC PRESSURE ON BASIC CELL

To evaluate the thermal resistance of the basic cell, the following steps should be taken:

- Calculate the relation between the apparent load on the cell and the contact load on the individual contact. This relation is found from static equilibrium.
- Break up the unit cell into contact regions and find the relation between the cell resistance and the resistance of a contact region.
- Calculate the thermal joint resistance for the contact region.
- Determine the apparent conductivity of the basic cell.

The following relation can be derived by considering the thermal resistance of a homogenous medium:

$$k_e = \frac{L_c}{R_c \; A_c} \tag{19}$$

where R_c is the resistance of the cell.

There is another resistance that arises as a result of the contact between the spheres and the plates of the container where thermal energy enters and exists the bed. We may call this the boundary resistance R_{BR}. Therefore, the total resistance of the packed bed is $R_{total} = R_{bed} + 2R_{BR}$ where the boundary resistances at both planes are assumed to be identical, see Fig. 9. The total effective thermal conductivity of a packed bed including the boundary resistance can be found from

$$k_{e,total} = \frac{L_{bed}}{A_c \left(R_{bed} + 2R_{BR}\right)} \tag{20}$$

where $R_{bed} = L_{bed} / \left(k_e \; A_c\right)$ and L_{bed} is the length of the bed in the heat transfer direction. It should be noted that the influence of the boundary resistance on the effective conductivity of the bed depends on the length of the bed and the diameter of the spheres. The boundary resistance has the same components as the joint resistance discussed in the previous section, see Fig. 3, and those relationships can be used to calculate the boundary resistance. It should be noted that because of the sphere-flat contact geometry of R_{BR}, the effective radius of curvature and the macrogap are different in R_{BR} than the ones used for the joint resistance between two spheres.

Simple Cubic (SC) Packing Cell

The geometry of the SC unit cell is shown in Figs. 2 and 9 where $b_L = \rho$, $A_c = D^2$, $L_c = D$, and $\rho = D/2$. Using the general contact region analysis, one can find the thermal joint resistance of the cell by applying Eq. (1) where the components R_s, R_L, R_g, and R_G can be calculated using Eqs. (3), (11), (16), and (17), respectively. The unit cell has one contact region thus $R_c = R_{j,SC}$. The effective thermal resistance of the SC packed beds is found from Eq. (19) as follows:

$$k_{e,SC} = \frac{1}{R_{j,SC} \; D} \tag{21}$$

Kitscha and Yovanovich [27] conducted experiments and investigated the solid and gas conduction for a contact between a sphere and a flat. The load on the contact was varied to study the effect of the applied load on the solid and gas conduction. For each load (or contact size) the gas pressure was varied from vacuum to atmospheric conditions. Two gases were used, air and argon, to study the effect of gas properties on the gas conduction. Two spherical carbon steel samples of radii 12.7 and 25.4 mm were chosen. The flat specimen was a steel 1020 with the surface roughness of $\sigma = 0.13$ μm and an effective microhardness $H_{mic} = 4$ GPa. Specimens were cylindrical with the same radius, $b_L = 12.7$ mm. To minimize the radiation and convection heat transfer to the surroundings, the lateral surfaces of the specimens were insulated. Figures 6 to 8 illustrates the comparison between the present model and Kitscha and Yovanovich [27] experimental data. The data show good agreement with the model. The relative RMS difference between the model and the data is approximately 7.2 percent.

As previously mentioned, Buonanno et al. [3] conducted experiments and measured the effective thermal conductivity of rough spherical packed beds. They tested beds of uniform sphere size which were packed in the SC and FCC arrangements. The spheres were stainless steel 100Cr6 of diameter 19.05 mm. Buonanno et al. [3] performed four tests with different surface roughness for each packing. The combined RMS surface roughness was varied from 0.03 to 1.7 μm. Their experimental apparatus and its properties

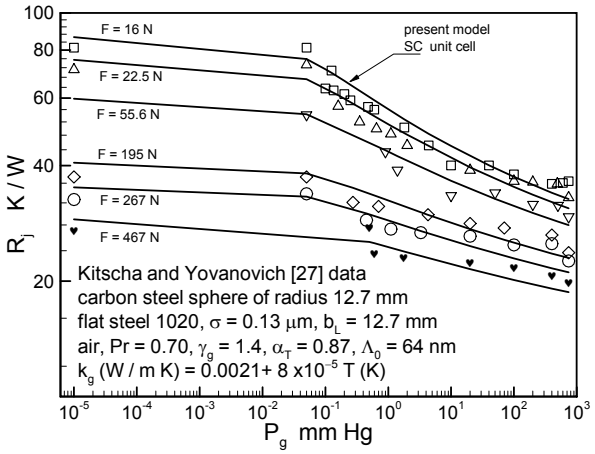

Figure 6. COMPARISON OF MODEL WITH KITSCHA AND YOVANOVICH 1974 DATA

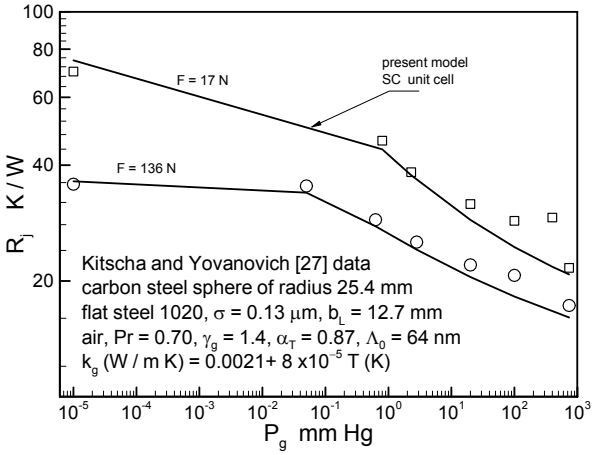

Figure 7. COMPARISON OF MODEL WITH KITSCHA AND YOVANOVICH 1974 DATA

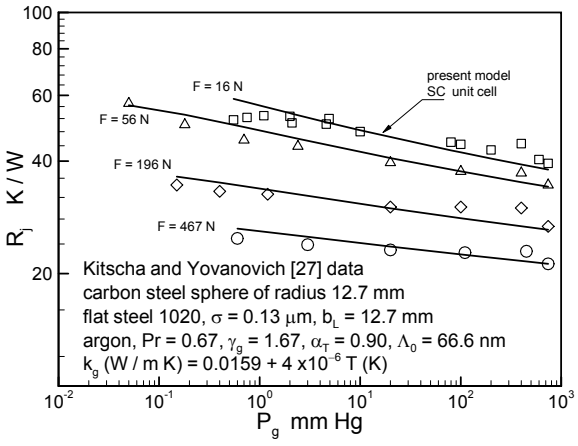

Figure 8. COMPARISON OF MODEL WITH KITSCHA AND YOVANOVICH 1974 DATA.

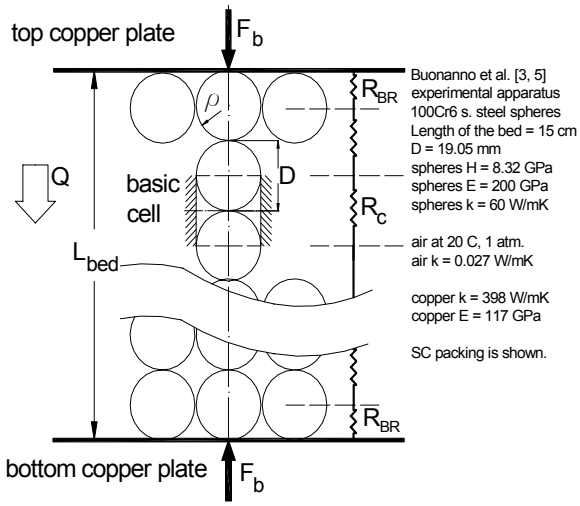

Figure 9. BUONANNO ET AL. 2003 EXPERIMENTAL APPARATUS FOR SC PACKING

are described in Fig. 9. Thermal energy enters the packed bed at the top copper plate and leaves the system at the bottom copper plate, two flux meters were used to measure the heat flow to the bed. The lateral sides of the bed were insulated to insure one-dimensional heat transfer. They reported an average contact load for each packing, which is the arithmetic mean of the structural weight of the spheres. Buonanno et al. [3] measured the total effective thermal conductivity of the bed which included the boundary thermal resistance R_{BR} at the top and bottom copper plates. To compare the present model with Buonanno et al.'s data [3], the total thermal resistance of their packed bed, described in Fig. 9, is calculated using Eq. (20) where the average contact load reported as 0.983 N is used. The comparison between the present model and Buonanno et al. [3] data is shown Fig. 10.

Buonanno et al. [5] using the same experimental apparatus described in Fig. 9, conducted experiments to study the effect of applied load on the effective thermal conductivity of packed beds. They reported the contact loads for two levels of combined surface roughness of 0.03 and 1.7 μm, without describing the method of applying the external load. The present model is compared with the reported data of [5] in Fig. 11. As shown both data sets show good

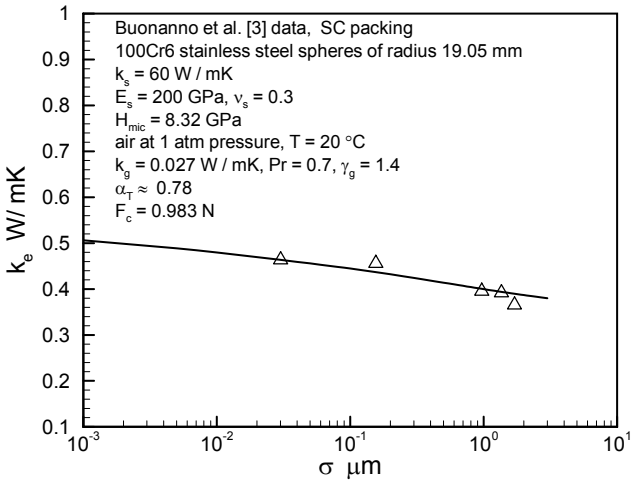

Figure 10. COMPARISON OF PRESENT MODEL WITH BUONANNO ET AL. 2003-A DATA, EFFECT OF ROUGHNESS SC PACKING

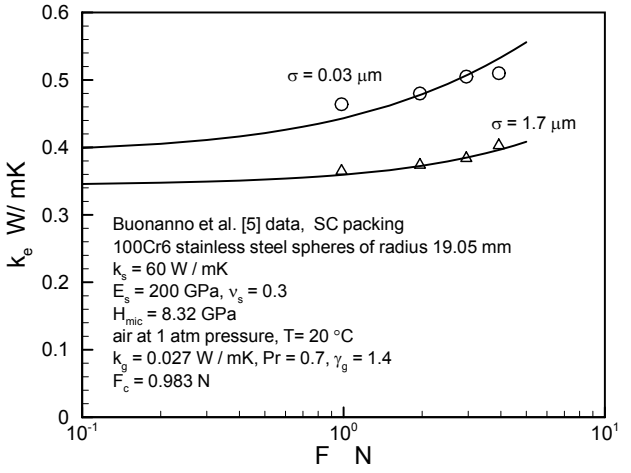

Figure 11. COMPARISON OF PRESENT MODEL WITH BUONANNO ET AL. 2003-B DATA, EFFECT OF APPLIED LOAD SC PACKING

agreement with the present model.

Face Centered Cubic (FCC) Packing Cell

A schematic geometry of the FCC unit cell is shown in Fig. 12 where 1/8th of the FCC cube shown in Fig. 1 is chosen, with $L_c = \sqrt{2}D/2$ and $A_c = D^2/2$. From symmetry, contact loads are identical. Assuming there are no frictional or tangential forces in contact regions, one can find a relationship between the apparent load on the cell cross section and the contact load $F_c = \sqrt{2}P_aD^2/8$.

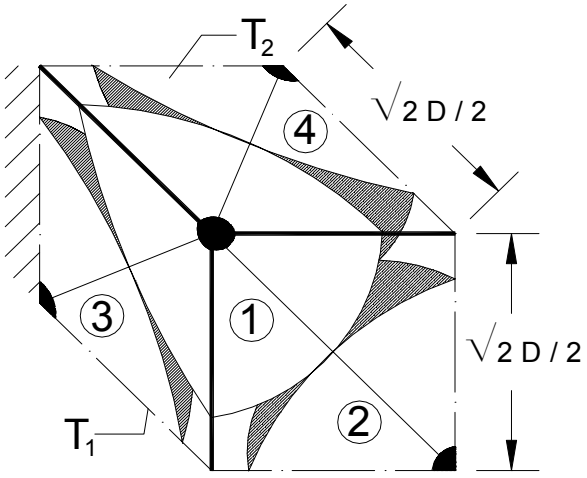

Figure 12. UNIT CELL FOR FCC PACKING

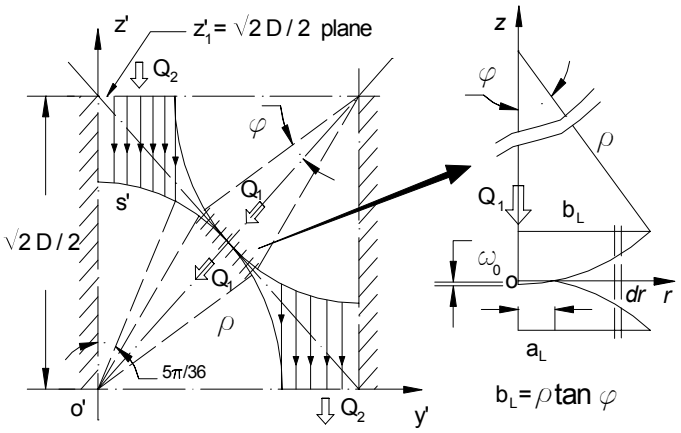

Figure 13. FCC CONTACT REGION, HEAT TRANSFER PATHS IN MACROGAP

A FCC packing contact region is shown in Fig. 13 where two 1/8 spheres make contact. For the FCC contact, the microcontact resistance R_s, the macrocontact resistance R_L, and the microgap resistance R_g can be calculated using Eqs. (3), (11), and (16), respectively. Since the thermal conductivity of solids are much larger than the gas thermal conductivity, the sphere surfaces can be assumed as isotherms. Also, the top and the bottom plates of the cell are isotherms. Therefore, the problem is reduced to finding the thermal resistance between these isotherms. We consider two parallel paths for conduction in the FCC macrogap. The first path is the heat transfer between two spheres, indicated by Q_1, in which Eq. (17) can be used with $b_L = \rho \tan \varphi$ to calculate R_{G1}. The angle φ is chosen arbitrarily to be 10° ($\pi/18$) by

considering the flow lines between two spheres, see Fig. 13. The second path is the heat transfer between the isothermal plane $z_1' = \sqrt{2}D/2$ and the isothermal sphere $s' = \rho\cos\phi$, indicated by Q_2, which can be found from

$$Q_2 = \int\int \frac{k_g \Delta T \cos\phi \; dA}{z_1' - s' + M} \tag{22}$$

where $dA = \rho^2 \sin\phi \, d\phi \, d\theta$ is a surface element on the sphere s', where $0 \le \phi \le 5\pi/36$, and $-\pi/4 \le \theta \le \pi/4$. Therefore, the thermal resistance for path Q_2 is

$$R_{G2} = \frac{1}{\pi k_g \rho \left[B \ln\left(\frac{B - 0.9036}{B - 1} \right) - 0.09369 \right]} \tag{23}$$

where $B = \sqrt{2} + M/\rho$. The heat transfer area corresponding to the path Q_1, a circle of radius b_L, is relatively small compared to the sphere surface area. This adds a constriction/spreading to the path Q_1 which can be estimated using Eq. (11), i.e., $R_{spread,G1} = 1/(2k_s b_L)$. Therefore, the macrogap thermal resistance for FCC is

$$\frac{1}{R_{G,FCC}} = \frac{1}{1/(2k_s b_L) + R_{G1}} + \frac{1}{R_{G2}} \tag{24}$$

Due to the relatively small gas layer thickness, most of the heat transfer occurs through the path Q_1; in other words $R_{G2} \gg R_{G1}$ thus Q_2 may be neglected with respect to Q_1. The macrogap thermal resistance for the FCC contact can be simplified to

$$R_{G,FCC} = R_{G1} + 1/(2k_s b_L) \tag{25}$$

With all the components of the joint resistance, the thermal contact resistance for a FCC contact region can be found from Eq. (1). As can be seen in Fig. 12, there are four parallel half-contact regions in the FCC unit cell. Thus, the thermal resistance of the unit cell is half of a FCC contact region, $R_c = R_{j,FCC}/2$. Using Eq. (19), the effective thermal resistance for FCC packed beds is

$$k_{e,\,FCC} = \frac{2\sqrt{2}}{R_{j,\,FCC}\; D} \tag{26}$$

The total effective thermal conductivity of the FCC bed, including boundary resistance, can be calculated using Eq. (20).

Buonanno et al. [3] measured the apparent conductivity of FCC packed beds with four levels of roughness and reported an average contact load (normal) without considering the effect of tangential/frictional forces in the contact area. The reported mean contact load is the mean structural weight of their FCC packed bed, $F_c = 0.78$ N.

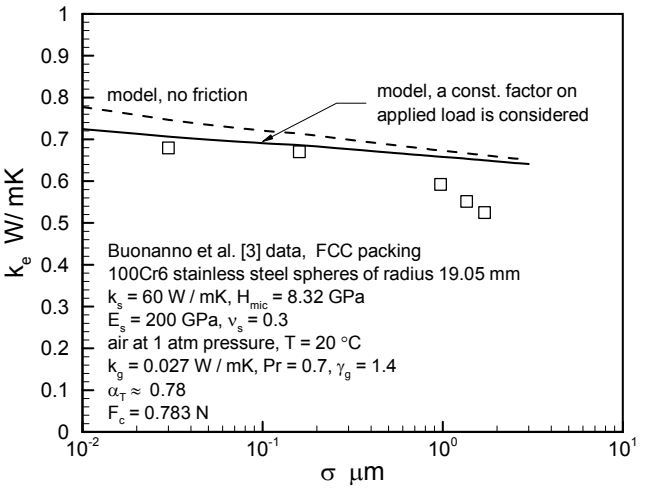

Figure 14. COMPARISON OF PRESENT MODEL WITH BUONANNO ET AL. 2003-A DATA, EFFECT OF ROUGHNESS FCC PACKING

Of course, the real normal contact loads in the bed could not be measured directly. Due to the frictional/tangential forces in the FCC contact area, normal loads which determine the macrocontact area, will be smaller than the reported value. As for the SC arrangement, the effect of frictional/tangential forces is small and therefore can be neglected.

As mentioned previously, the contact mechanics of the present model do not account for tangential forces in the contact area corresponding to the friction between the contacting spheres. Considering the effect of friction on the contact load is a complex task and requires knowledge of the friction factor(s) between the spheres in the packed bed. Therefore, a quantitative comparison between the present model and the data of [3] is impossible. However, a qualitative comparison which shows the trends of the model and the data is presented in Fig. 14. Two curves are shown for the model. The dashed line in which the reported contact load is used, i.e., $F_c = 0.78$ N. The solid curve represents the model in which a constant factor of 0.5 (arbitrary) is applied to the reported contact load to account for the friction between spheres. As expected, the difference between the data and the model is larger at higher roughness values which indicates that the effect of friction is more significant at higher roughness values.

The present model is also compared with Buonanno et al. data [5] where the effect of contact load on the effective thermal conductivity was experimentally investigated. Two sets of data were collected for two levels of combined surface roughness, i.e., 0.03 and 1.7 μm as the applied load was

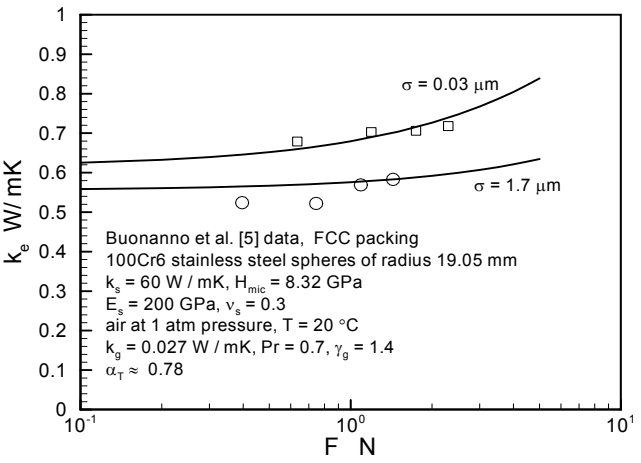

Figure 15. COMPARISON OF PRESENT MODEL WITH BUONANNO ET AL. 2003-B DATA, EFFECT OF LOAD FCC PACKING

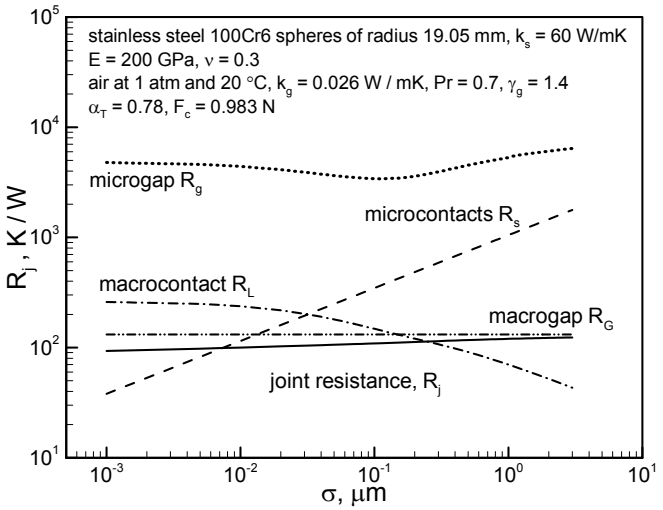

Figure 16. EFFECT OF ROUGHNESS OF JOINT RESISTANCE AND ITS COMPONENTS, SC CONTACT REGION

varied [5]. As discussed above, two constants were considered on the reported contact loads to account for the effect of the tangential/frictional forces on the macrocontact, i.e., 0.8 and 0.5 for 0.03 and 1.7 μm surface roughness data, respectively. As shown in Figs. 14 and 15, the model shows the trend of the data. It also can be concluded that the effect of frictional forces becomes more important as the surface roughness increases.

PARAMETRIC STUDY

The proposed model can be used to investigate the influence of important parameters/properties of a packed bed on its effective thermal conductivity. The trends predicted by the present model, as roughness and the contact load vary, are shown in the previous section for both SC and FCC packing where the model is compared with the experimental data. In this section, the effect of the gas type and gas pressure and the relative size of spheres on the bed thermal conductivity are investigated. Since, the trends of both packing arrangements, i.e. SC and FCC, are similar only the SC packing results are presented.

The influence of roughness on the SC joint resistance and its components predicted by the model is shown in Fig. 16. The same input parameters/properties of the SC packed bed of [3] is used, see Fig. 9. As roughness is increased, while other contact parameters listed in Fig. 16 are held constant, it can be seen that i) the microcontacts resistance R_s increases linearly, see Eq. (3), ii) the contact load spreads over a larger area or the macrocontact area increases which leads to a lower macrocontact resistance R_L, iii) as a result of larger macrocontact area, the macrogap area becomes smaller thus the macrogap resistance R_G becomes higher (slightly in this case); also it can be observed that most of the heat transfer occurs through the macrogap, and iv) the microgap resistance R_g is very high and can be neglected. Another interesting trend can be observed in the microgap resistance R_g. As roughness decreases, the separation between two spheres in the macrocontact area decreases, i.e., the size of the microgaps becomes smaller, see Fig. 2, which has a decreasing effect on R_g. Also with smaller microgaps, the rarefaction effect in the microgaps becomes more important which leads to an increase in the microgap resistance R_g. As a result of these two competing effects, the microgap resistance R_g decreases to a certain point and then approaches its limit where roughness is zero, as shown in Fig. 16. This limit can be found from Eq. (16)

$$\lim_{\sigma \to 0} R_g = \frac{M}{\pi k_g \; a_H^2} \tag{27}$$

where a_H is the Hertzian contact radius. It should be noted that for smooth surfaces the microcontacts resistance $R_s = 0$ and since R_s and R_g are in parallel, Eq. (1), the value of R_g does not change the joint resistance. The trend seen in Fig. 16 for the joint resistance is consistent with the experimental data of [3].

Figure 17 illustrates the effect of the interstitial gas type and the gas pressure on the effective thermal conductivity of the same packed bed described above, with a surface roughness $\sigma = 0.5$ μm. Two different gases, air and helium, are chosen for the comparison since their thermal conductivities

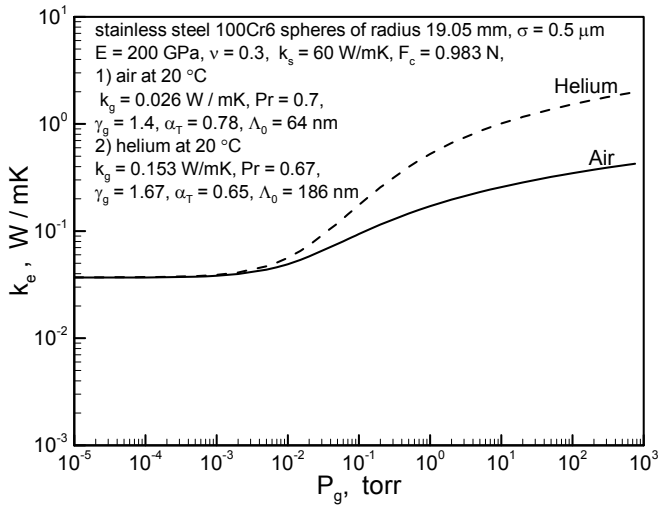

Figure 17. EFFECT OF GAS TYPE AND PRESSURE ON EFFECTIVE THERMAL CONDUCTIVITY OF SC ARRANGEMENT

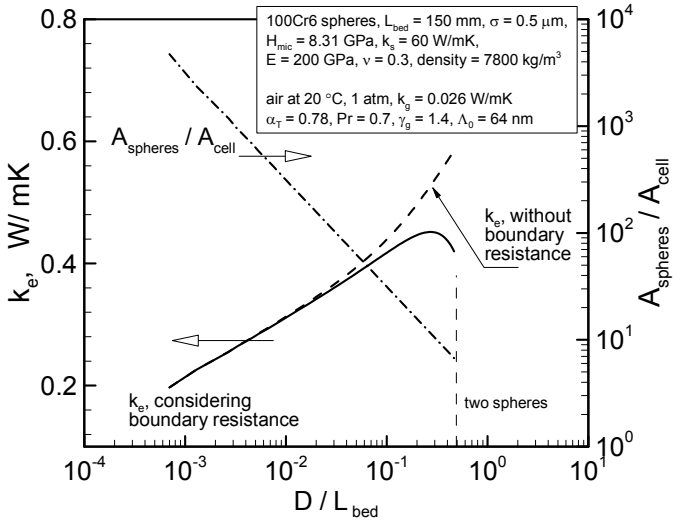

Figure 18. EFFECT OF PARTICLE RADIUS ON EFFECTIVE THERMAL CONDUCTIVITY OF SC PACKED BEDS

cover a wide range, i.e., 0.026 and 0.153 W/mK for air and helium, respectively. For each gas the gas pressure is varied from vacuum 10^{-5} to atmospheric pressure 760 $torr$, see Fig. 17 for the bed and gases properties. It can be seen that in a vacuum and very low gas pressures thermal conductivities of both beds are identical. As expected, with increasing gas pressure the bed filled with helium shows higher effective conductivity, a factor of 4.7 higher at atmospheric pressure.

The variation of the effective thermal conductivity of a SC packed bed, the same bed as described above, versus the relative diameter of spheres D/L_{bed} is presented in Fig. 18. The average contact load for each sphere diameter value is considered as half of the weight of the stack of spheres in a packed bed of 150 mm length and the density of 100Cr6 spheres is assumed to be 7800 kg/m^3. All other input parameters are held constant as the diameter of spheres is varied over the range of $0.1 \leq D \leq 75$ mm, i.e., $0.0007 \leq D/L_{bed} \leq 0.5$, see Fig. 18 for other input parameters. As shown, the effective thermal conductivity increases as the diameter of the spheres increases. This is a direct result of decreasing the total relative surface area of the spheres in the packed bed $A_{spheres}/A_{cell}$ and increasing the mean contact load. In addition, the variation of the ratio $A_{spheres}/A_{cell}$ as a function of the relative size of the spheres is shown in Fig. 18.

The effect of boundary resistance on the effective thermal conductivity of the bed is also shown in Fig. 18. The boundary resistance is calculated as discussed in Eq. (20). Two curves are shown in the plot, the boundary resistance is considered in calculating the solid curve and it is neglected in the dashed curve. As shown, the effect of the boundary resistance is relatively small where the relative size of the spheres are small.

SUMMARY AND CONCLUSIONS

Analytical solutions for steady-state conduction heat transfer in regularly packed beds of rough spheres with a uniform diameter in the presence of a stagnant gas are developed. SC and FCC packing are studied since they present the upper and lower bounds for the effective thermal conductivity of randomly packed beds. Compact relationships are derived for calculating the effective thermal conductivities of SC and FCC unit cells. These models account for the thermophysical properties of spheres and the gas, contact load, spheres diameter, spheres roughness and slope, and temperature and pressure of the gas.

Experimental data [27] collected for a SC basic cell are compared with the model. The data are collected at different applied loads where at each load the gas pressure is varied from vacuum to atmospheric pressure. Experiments include two diameters of stainless steel spheres with argon and air as interstitial gas. The present model shows very good agreement with the data of [27] with the RMS difference in the order of 7 percent.

The present model is also compared with experimental data collected by Buonanno et al. [3] and [5] for SC and FCC regularly packed beds. The data include a range of the contact load and the surface roughness of the single-sized stainless steel spheres in air at atmospheric condition. The

present model shows excellent agreement with the SC data. Due to the frictional/tangential forces in the FCC contact region, the present model can not be compared quantitatively with the FCC data. However, the model shows the trend of the FCC data in a qualitative comparison.

The influence of the surface roughness on the joint resistance predicted by the model and its components are presented and their trends are discussed. It is shown that most of the heat transfer occur through the macrogap. Effects of the gas type and pressure and the relative size of the spheres on the effective thermal conductivity of the beds are studied. It is observed that the thermal conductivity of the packed beds increase by increasing the relative diameter of the spheres. The influence of the boundary resistance on the conductivity of packed beds is investigated. It is seen that for an uncompressed packed bed, the effect of boundary resistance is negligible where the ratio of the spheres diameter over the bed length is approximately 0.02.

ACKNOWLEDGMENT

The authors gratefully acknowledge the financial support of the Centre for Microelectronics Assembly and Packaging, CMAP and the Natural Sciences and Engineering Research Council of Canada, NSERC.

REFERENCES

[1] S. Kikuchi, T. Kuroda, and M. Enoeda, "Preliminary thermo-mechanical analysis of iter breeding blanket," *JAERI Tech. 98-059*, 1999.

[2] C. L. Tien and K. Vafai, "Statistical bounds for the effective thermal conductivity of microsphere and fibrous insulation," *AIAA Progress Series*, vol. 65, pp. 135–148, 1979.

[3] G.Buonanno, A. Carotenuto, G. Giovinco, and N. Massarotti, "Experimental and theoretical modeling of the effective thermal conductivity of rough steel spheroid packed beds," *Journal of Heat Transfer, ASME*, vol. 125, pp. 693–702, 2003.

[4] G.Buonanno and A. Carotenuto, "The effective thermal conductivity of packed beds of spheres for a finite contact area," *Numerical Heat Transfer*, vol. 37, pp. 343–357, 2000.

[5] G.Buonanno, A. Carotenuto, G. Giovinco, and N. Massarotti, "Effective thermal conductivity of rough spheres packed beds," *Proceedings of HT2003, ASME Heat Transfer Conference, July 21-23, Las Vegas, Nevada, USA, Paper No. HT2003-47130*, 2003.

[6] A. J. Slavin, F. A. Londry, and J. Harrison, "A new model for the effective thermal conductivity of packed beds of solid spheroids: Alumina in helium between 100 and 500 c," *Journal of Heat and Mass Transfer*, vol. 43, 2000.

[7] Y. Ogniewicz and M. M. Yovanovich, "Effective conductivity of regularly packed spheres: Basic cell model with constriction," *Heat Transfer and Thermal Control Systems, Editor L. S. Fletcher, Progress in Astronautics and Aeronautics AIAA, New York*, vol. 60, 1978.

[8] P. J. Turyk and M. M. Yovanovich, "Modified effective conductivity models for basic cells of simple cubic packed beds," *Proc. 23rd National Heat Transfer Conference, Aug. 4-7, Denver, Colorado, HTD*, vol. 46, pp. 9–19, 1984.

[9] M. M. Yovanovch and E. E. Marotta, *Thermal Spreading and Contact Resistances*, ch. 4. Hoboken, New York, USA: Heat Transfer Handbook, Editors: A. Bejan and D. Kraus, John Wiley and Sons Inc., 2003.

[10] V. S. Arpaci and P. S. Larsen, *Convection Heat Transfer*, ch. 4. Englewood Cliffs, New Jersey 07632, USA: Prentice-Hall Inc., 1984.

[11] J. A. Greenwood and B. P. Williamson, "Contact of nominally flat surfaces," *Proc., Roy. Soc., London, A295*, pp. 300–319, 1966.

[12] M. Bahrami, J. R. Culham, M. M. Yovanovich, and G. E. Schneider, "Review of thermal joint resistance models for non-conforming rough surfaces in a vacuum," *Paper No. HT2003-47051, ASME Heat Transfer Conference, July 21-23, Las Vegas, Nevada*, 2003.

[13] M. G. Cooper, B. B. Mikic, and M. M. Yovanovich, "Thermal contact conductance," *International Journal of Heat and Mass Transfer*, vol. 12, pp. 279–300, 1969.

[14] M. Bahrami, J. R. Culham, and M. M. Yovanovich, "A scale analysis approach to thermal contact resistance," *Paper No. IMECE2003-44097, ASME International Mechanical Enginnering Congress and RD Exp, Nov. 15-21, Washington D.C., USA*, 2003.

[15] M. M. Yovanovich and A. Hegazy, "An accurate universal contact conductance correlation for conforming rough surfaces with different micro-hardness profiles," *AIAA, Paper No. 83-1434*, 1983.

[16] M. R. Sridhar and M. Yovanovich, "Empirical methods to predict vickers microhardness," *Wear*, vol. 193, pp. 91–98, 1996.

[17] M. Bahrami, M. M. Yovanovich, and J. R. Culham, "A compact model for spherical rough contacts," *Paper No. TRIB2004-64015, ASME/ STLE International Joint Tribology Conference, October 24-27, Long Beach, California, USA*, 2004.

[18] K. L. Johnson, *Contact Mechanics*. Cambridge, UK.: Cambridge University Press, 1985.

[19] J. A. Greenwood and J. H. Tripp, "The elastic contact of rough spheres," *Transactions of the ASME: Journal of Applied Mechanics*, vol. 89, no. 1, pp. 153–159, 1967.

[20] J. A. Greenwood, K. L. Johnson, and M. Matsubara, "A surface roughness parameter in hertz contact," *Wear*, vol. 100, pp. 47–57, 1984.

[21] M. M. Yovanovich, G. E. Schneider, and C. H. Tien, "Thermal resistance of hollow spheres subjected to arbitrary flux over their poles," *Paper No. 78-872, 2nd AIAA/ASME Thermophysics and Heat Transfer Conference, May 24-26, Palo Alto, California*, 1978.

[22] G. S. Springer, "Heat transfer in rarefied gases," *Advances in Heat Transfer, Edited by Irvine T. F. and Hartnett J. P.*, vol. 7, pp. 163–218, 1971.

[23] E. H. Kennard, *Kinetic Theory of Gases*. New York, London: McGraw-Hill, 1938.

[24] S. Song and M. M. Yovanovich, "Correlation of thermal accomodation coefficient for engineering surfaces," *National Heat Transfer Conference, Pittsburgh, PA, August 9-12*, 1987.

[25] M. Bahrami, J. R. Culham, and M. M. Yovanovich, "Thermal resistances of gaseous gap for non-conforming rough contacts," *AIAA Paper No. 2004-0822, 42nd AIAA Aerospace Meeting and Exhibit, Jan 5-8, Reno, Nevada*, 2004.

[26] M. Bahrami, J. R. Culham, and M. M. Yovanovich, "Thermal resistances of gaseous gap for conforming rough contacts," *AIAA Paper No. 2004-0821, 42nd AIAA Aerospace Meeting and Exhibit, Jan 5-8, Reno, Nevada*, 2004.

[27] W. W. Kitscha and M. M. Yovanovich, "Experimental investigation on the overall thermal resistance of sphere-flat contacts," *Progress in Astronautics and Aeronautics: Heat Transfer with Thermal Control Applications, Vol.39, p93, Also AIAA paper 74-13*, 1974.